Computational and Structural Biotechnology Journal 17 (2019) 963–971

COMPUTATIONAL AND STRUCTURAL BIOTECHNOLOGY JOURNAL

journal homepage: www.elsevier.com/locate/csbj

Human Albumin Impairs Amyloid β-peptide Fibrillation Through its C-terminus: From docking Modeling to Protection Against Neurotoxicity in Alzheimer's disease

Pol Picón-Pagès [a,1], Jaume Bonet [b,1], Javier García-García [b], Joan Garcia-Buendia [a], Daniela Gutierrez [c], Javier Valle [d], Carmen E.S. Gómez-Casuso [a], Valeriya Sidelkivska [a], Alejandra Alvarez [c], Alex Perálvarez-Marín [e], Albert Suades [e], Xavier Fernàndez-Busquets [f,g], David Andreu [d], Rubén Vicente [a], Baldomero Oliva [b,*], Francisco J. Muñoz [a,*]

[a] Laboratory of Molecular Physiology, Faculty of Health and Life Sciences, Universitat Pompeu Fabra, Barcelona, Spain
[b] Laboratory of Structural Bioinformatics (GRIB), Faculty of Health and Life Sciences, Universitat Pompeu Fabra, Barcelona, Spain
[c] Cell Signaling Laboratory, Centro UC de Envejecimiento y Regeneración (CARE), Department of Cellular and Molecular Biology, Biological Sciences Faculty, Pontificia Universidad Católica de Chile, Santiago, Chile
[d] Laboratory of Proteomics and Protein Chemistry, Faculty of Health and Life Sciences, Universitat Pompeu Fabra, Barcelona, Spain
[e] Unitat de Biofísica, Departament de Bioquímica i de Biologia Molecular, Facultat de Medicina, Centre d'Estudis en Biofísica, Universitat Autònoma de Barcelona, Barcelona, Spain
[f] Nanomalaria Group, Institute for Bioengineering of Catalonia (IBEC), The Barcelona Institute of Science and Technology, Baldiri Reixac 10-12, ES-08028 Barcelona, Spain
[g] Barcelona Institute for Global Health (ISGlobal, Hospital Clínic-Universitat de Barcelona), Rosselló 149-153, ES-08036 Barcelona, Spain

ARTICLE INFO

Article history:
Received 18 January 2019
Received in revised form 3 June 2019
Accepted 13 June 2019
Available online 26 June 2019

Keywords:
Alzheimer's disease
Amyloid
Albumin
β-Sheet
Docking

ABSTRACT

Alzheimer's disease (AD) is a neurodegenerative process characterized by the accumulation of extracellular deposits of amyloid β-peptide (Aβ), which induces neuronal death. Monomeric Aβ is not toxic but tends to aggregate into β-sheets that are neurotoxic. Therefore to prevent or delay AD onset and progression one of the main therapeutic approaches would be to impair Aβ assembly into oligomers and fibrils and to promote disaggregation of the preformed aggregate. Albumin is the most abundant protein in the cerebrospinal fluid and it was reported to bind Aβ impeding its aggregation. In a previous work we identified a 35-residue sequence of clusterin, a well-known protein that binds Aβ, that is highly similar to the C-terminus (CTerm) of albumin. In this work, the docking experiments show that the average binding free energy of the CTerm-$A\beta_{1-42}$ simulations was significantly lower than that of the clusterin-$A\beta_{1-42}$ binding, highlighting the possibility that the CTerm retains albumin's binding properties. To validate this observation, we performed *in vitro* structural analysis of soluble and aggregated 1 μM $A\beta_{1-42}$ incubated with 5 μM CTerm, equimolar to the albumin concentration in the CSF. Reversed-phase chromatography and electron microscopy analysis demonstrated a reduction of $A\beta_{1-42}$ aggregates when the CTerm was present. Furthermore, we treated a human neuroblastoma cell line with soluble and aggregated $A\beta_{1-42}$ incubated with CTerm obtaining a significant protection against Aβ-induced neurotoxicity. These *in silico* and *in vitro* data suggest that the albumin CTerm is able to impair Aβ aggregation and to promote disassemble of Aβ aggregates protecting neurons.

Abbreviations: AD, Alzheimer's disease; APP, amyloid precursor protein; Aß, Amyloid-ß peptide; CD, Circular dichroism; CSF, cerebrospinal fluid; CTerm, albumin C-terminus; f$A\beta_{1-42}$, HiLyte Fluor488 labelled human $A\beta_{1-42}$; HPLC, high performance liquid chromatography; LC-MS, Liquid chromatography-mass spectrometry; MTT, 3-(4,5-dimethylthiazol-2-yl)-2,5-diphenyltetrazolium bromide; NMR, nuclear magnetic resonance; PBS, phosphate-buffered saline; PDB, Protein Data Bank; PPI, protein-protein interactions; SDS, sodium dodecyl sulfate; TEM, transmission electron microscopy; TFA, trifluoroacetic acid; UV, ultraviolet.

* Corresponding authors.
E-mail addresses: pol.picon_pages@outlook.es (P. Picón-Pagès), jaume.bonet@gmail.com (J. Bonet), javigx2@gmail.com (J. García-García), joan.garcia04@estudiant.upf.edu (J. Garcia-Buendia), dngutierrez@uc.cl (D. Gutierrez), javier.valle@upf.edu (J. Valle), csgomezcasuso@gmail.com (C.E.S. Gómez-Casuso), valeriesidelkivska@gmail.com (V. Sidelkivska), aalvarez@bio.puc.cl (A. Alvarez), Alex.Peralvarez@uab.cat (A. Perálvarez-Marín), albert.suades@dbb.su.se (A. Suades), xfernandez_busquets@ub.edu (X. Fernàndez-Busquets), david.andreu@upf.edu (D. Andreu), ruben.vicente@upf.edu (R. Vicente), baldo.oliva@upf.edu (B. Oliva), paco.munoz@upf.edu (F.J. Muñoz).
[1] These authors have contributed equally to the present work.

https://doi.org/10.1016/j.csbj.2019.06.017

1. Introduction

Alzheimer's disease (AD) histopathological hallmarks are the extracellular aggregation of amyloid β-peptide (Aβ) in the brain, and the intraneuronal aggregation of hyperphosphorylated tau protein [1,2]. The amyloid cascade hypothesis proposes that Aβ aggregation into oligomers and fibrils induces synaptotoxicity and ultimately neuronal death [3–5].

The Aβ is a ~4 kDa peptide released from the amyloid precursor protein (APP) [6] by the sequential action of the enzymes β- and γ-secretases [7,8]. Aβ is produced thoughout the life of an individual, being physiologically degraded in the brain by different enzymes or cleared through the blood brain barrier into the blood [9]. During aging there is an increase in Aβ production and an impairment of Aβ clearance from brain to blood [10], favoring its aggregation into β-sheets. Then, Aβ forms oligomers known to be highly neurotoxic [3,4], and they progress into forming amyloid fibrils that are packed into senile plaques.

At present, AD prevalence is increasing as the world population ages [11] and has become a major health and social problem expected to reach pandemic status by 2050 [12]. Unfortunately, despite the current knowledge on APP processing, there are no treatments that effectively prevent AD development or its progression. On the other hand, the use of antibodies against Aβ to disassemble cerebral Aβ aggregates [13–15] has not yielded positive results in clinical trials.

Interestingly, clusterin (also termed apolipoprotein J) and albumin are cerebral proteins that have been reported to bind Aβ under physiological conditions [16–18]. In fact, clusterin impairs Aβ aggregation in the brain [16] and some clusterin polymorphisms are major risk factors for late onset AD [19]. Albumin has also been demonstrated to inhibit Aβ aggregation [20–23]. These findings make the study of clusterin and albumin of high relevance to understand AD etiology and to elucidate mechanisms of neuroprotection in AD.

Albumin is the most abundant protein in the cerebrospinal fluid (CSF) produced mostly by ultrafiltrate of plasma proteins [24] and minimally by the microglia [25]. It is a single peptide chain of 585 amino acids with a secondary structure containing 67% α-helix, 23% extended chain and 10% β-sheet [26–28]. Albumin is a flexible molecule, with the ability to change its structure depending on environmental conditions such as temperature, pH or ionic strength [29,30]. It can bind a plethora of different molecules [30–33], and it can even act as a free radical scavenger [34]. More specifically, albumin can bind Aβ [20,35,36] and is responsible for 95% of its transport in the blood [18,37,38], thereby regulating the amount of circulating Aβ.

Previously, we used the Protein-Protein Interface Prediction Server (iFRAG) to predict the interaction for short protein fragments and found that clusterin shares a common sequence with the C-terminus domain of human albumin (CTerm; Fig. S1) [39]. Here, we address the effect of its CTerm in Aβ aggregation using *in silico* and *in vitro* techniques.

Computational methods to predict and evaluate protein-protein interactions (PPIs) represent a feasible alternative to experimental approaches. Although docking experiments are currently used to predict the conformation of PPIs [40], it has been shown that the distribution of scores of different docking populations could be used to discern between interacting and non-interacting protein pairs. This is valid even when the native conformation cannot be identified among the poses [41] and the population of docking poses can be used to predict the binding energy if the structure of the complex is unknown [42]. In this work, we used similar principles to assess the binding potential of clusterin, albumin and the CTerm to the alpha and beta conformations of the $A\beta_{1-42}$ peptide. We focused our efforts on elucidating the physiological relevance of the CTerm and its interaction with $A\beta_{1-42}$ peptide by *in vitro* experiments using different techniques and cell cultures.

2. Methodology

2.1. Modeling of the Clusterin Peptide

We found the four homologous sequences between clusterin and albumin in a previous work through sequence alignments [39]. Due to the lack of available structures for clusterin or the peptide region of interest, 5 decoys of the most promising peptide according to iFrag [39] were built with MODELLER [43–45] following the alignment shown in Fig. 1A. The five decoys were minimized and scored with Rosetta [46] and the best-scored decoy was selected as the structural representative of the clusterin-peptide (Fig. 1B).

2.2. $A\beta_{1-42}$ -Docking Analyses

With the exception of the clusterin-peptide model, structures for all the different elements required for the docking analyse were obtained from the Protein Data Bank (PDB) [47]. The clusterin-peptide and the CTerm structure (crystal structure PDB ID: 5FUO [48], residues 504-538) were docked with two different target binders: (1) the $A\beta_{1-42}$ α conformation (nuclear magnetic resonance (NMR) ensemble PDB ID: 1IYT [49]), (2) the $A\beta_{1-42}$ β conformation (cryo-EM structure PDB ID: 5OQV [50]). Additionally, CTerm was also docked to the most terminal region of albumin (PDB ID: 5FUO, residues 539-582). to which is normally bound (CTerm-lid). This region of the wild-type albumin hides the putative recognition site between CTerm and $A\beta_{1-42}$ (Fig. 2A).

From the only two available NMR structures in the PDB [47] presenting the full 42 residues of the $A\beta_{1-42}$ peptide, we selected 1IYT over 1Z0Q [doi:https://doi.org/10.1002/cbic.200500223] (see alignment of resolved residue densities for all $A\beta_{1-42}$ peptides in the PDB at https://github.com/structuralbioinformatics/amyloid/blob/master/albumina/source/alpha_amyloids/alignment.highlight.aln) for two main reasons. On the one hand, most of the standard PDB metric qualities (namely clashscore, Ramachandran outliers and sidechain outliers) are far better in 1IYT than in 1Z0Q. On the other hand, 1Z0Q is described as an intermediate state between the α and β conformations of $A\beta_{1-42}$ while 1IYT aims to represent the stable alpha state of the peptide.

For each pair, a total of 8000 decoys were generated with Rosetta's docking protocol [51] and optimized with Rosetta's FastRelax [52]. Decoys were analyzed in terms of their ddG, shape complementarity and structural variation of the target binder.

2.3. CTerm Synthesis

The CTerm peptide, AETFTFHADICTLSEKERQIKKQTALVELVKHKPK-amide, containing the hydrophobic domains reported to be Aβ binding sites by García et al. [39] was produced in C-terminal carboxamide form by Fmoc solid phase synthesis in a peptide synthesizer Prelude (Gyros Protein Technologies). It was purified to near homogeneity (97%) by reversed-phase high performance liquid chromatography (HPLC).

2.4. CTerm Analysis

Analytical reversed-phase HPLC was performed on C18 columns (4.6 × 50 mm, 3 μm; Phenomenex) in a liquid chomatrograph (LC-2010A; Shimadzu). Solvent A was 0.045% trifluoroacetic acid (TFA) in H_2O; solvent B was 0.036% TFA in acetonitrile. Elution was carried out with linear 15–50% gradients of solvent B into A over 15 min at 1 mL/min flow rate, with UV detection at 220 nm. LC-mass spectrometry (MS) was performed in a LC-MS 2010EV instrument (Shimadzu) fitted with an XBridge column (4.6 × 150 mm, 3.5 μm; Waters), eluted with

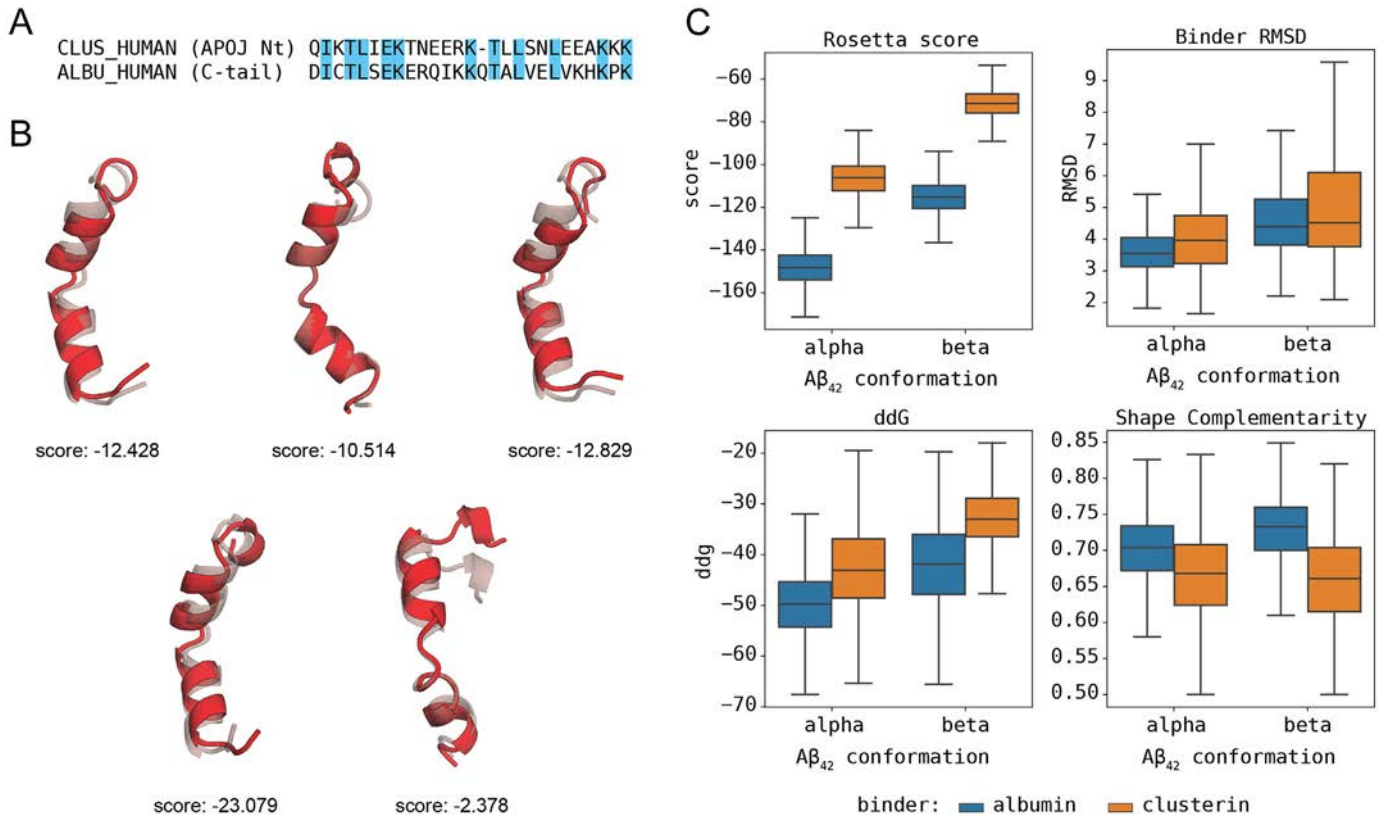

Fig. 1. *In silico* modeling of clusterin and docking comparison with the CTerm. A) Guiding alignment for the modeling of the clusterin peptide. Common amino acids are labelled in blue. B) Structures of the 5 clusterin decoys with the initial models (transparent) and the minimized structure (red). Rosetta scores for the minimized structure are shown under each structure. C) Comparison of scores between the docking population of clusterin (or albumin) and the $A\beta_{1-42}$ peptide (in α or β conformation). Using a total of 8000 decoys on each docking population, the scores of albumin peptides systematically outperforms those of clusterin when binding the same target, with a statistical significance of $p < .001$.

a 15–50% linear gradient of B into A (A = 0.1% formic acid in H_2O; B = 0.08% formic acid in acetonitrile) over 15 min at a flow rate of 1 mL/min, with UV detection at 220 nm.

2.5. CTerm Purification

Preparative HPLC runs were performed on a Luna C18 column (21.2 mm × 250 mm, 10 μm; Phenomenex), using linear 15–50% gradients of solvent B (0.1% in acetonitrile) into A (0.1% TFA in H_2O), as required, with a flow rate of 25 mL/min. Fractions of high (>95%) HPLC homogeneity were further characterized by electrospray mass spectrometry using a XBridge column C18 (Waters) and a gradient at 1 mL/min of A (0.1% formic acid in H_2O) into B (0.08% formic acid in CH_3CN). Detection was performed at 220 nm. Fractions of adequate homogeneity and with the expected mass (4067.77 Da) were combined, lyophilized, and used in subsequent experiments. See Figs. S2 and S3 and Table S1 for additional details.

2.6. Circular Dichroism (CD)

CTerm was dissolved in 5 mM NaOH at a stock concentration of 1 mg/mL. The peptide was further dissolved to yield a 50 mM concentration in 10 mM phosphate buffer at pH 7.2 in the presence or absence of 20 mM SDS. The CD was performed as follows. The spectral region was recorded from 190 to 250 nm, with a 0.5 nm step resolution, on a Jasco J-715 CD spectropolarimeter (Jasco Inc.) using a quartz cell of 1.0 mm optical path length at room temperature. The scanning speed was 100 nm/min with 2 s time response, and the spectra were collected and averaged over 10 scans. Secondary structure estimation derived from CD data was assessed using K2D3 [53].

2.7. Amyloid Preparation

Lyophilized $A\beta_{1-42}$ (Anaspec) was solubilized as previously described [54]. Briefly, 1 mg Aβ was dissolved in 250 μL of MilliQ water and pH was adjusted to ≥10.5 using 1 M NaOH solution to avoid the isoelectric point of Aβ disassembling and aggregates that may be present. Peptides were diluted in 250 μL of 20 mM phosphate buffer (pH 7.4). Furthermore, the solutions were sonicated for 1 min in a bath-type sonicator (Bioruptor, Diagenode). The preparations were immediately used for aggregation or stored in 25 μL aliquots at −20 °C until used.

2.8. Reversed-Phase Chromatography Analysis of CTerm Effect on Aβ Aggregation

Soluble and pre-aggregated (24 h at 37 °C) 1 μM $A\beta_{1-42}$ was dissolved in Ham's F12 medium and incubated in the presence/absence of 5 μM CTerm at 37 °C during 24 h for assembly and disassemble assays. Samples were quenched in 2% trifluoroacetic acid and injected in a Waters 2690 HPLC coupled to a UV detector set to 214 nm. A linear gradient of 25%–45% of 0.1% trifluoroacetic acid in acetonitrile was applied for 90 min into a 250 × 4.6 mm (5 μm) C4 column at a flow rate of 0.75 mL/min.

2.9. Reversed-Phase Chromatography Analysis of Control Peptide Effect on Aβ Aggregation

Random peptides with the same size that CTerm were synthetized: peptides X, Y and Z. Soluble and pre-aggregated (24 h at 37 °C) 1 μM Aβ1–42 was dissolved in Ham's F12 medium and incubated in the presence/absence of 5 μM peptides at 37 °C during 24 h for assembly and

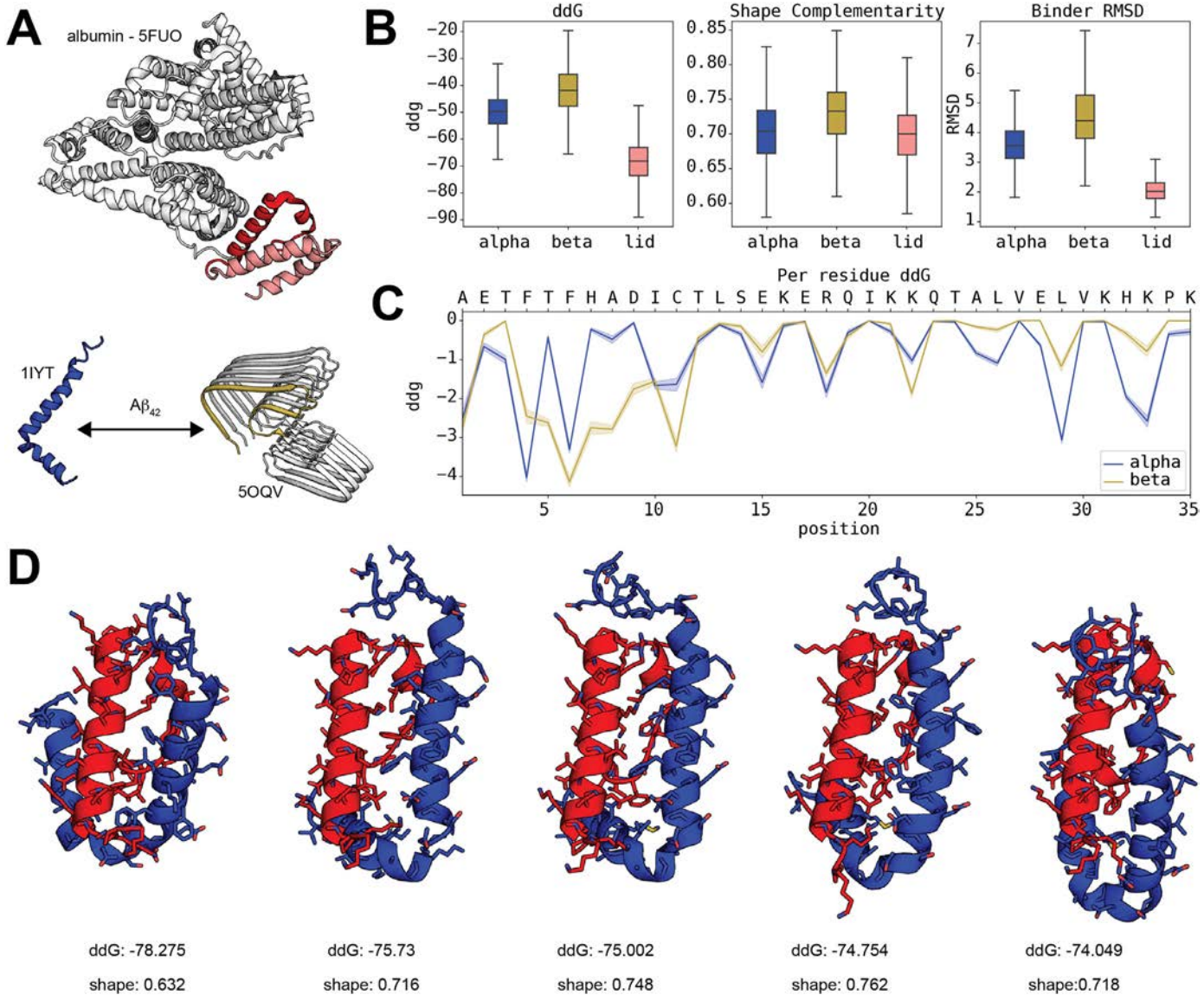

Fig. 2. Structural *in silico* analysis of $A\beta_{1-42}$ interaction with the CTerm. A) Structure of human albumin. The sequence of the CTerm is labelled in red. The continuing structural segment (CTerm-lid) is shown in pink (top). The α and β configurations of $A\beta_{1-42}$ are shown at the bottom. B) Scores distribution of the docking analysis of CTerm against α-$A\beta_{1-42}$, β-$A\beta_{1-42}$, and CTerm-lid. C) Individual contribution of the residues of the CTerm to the binding according to the top 200 decoys (2.5% of the total). D) Representation of the first five top-scored decoys of the docking between the amyloid peptide (blue) and the CTerm (red). ddG score and shape complementarity are provided under each structure.

disassemble assays. Analytical reversed-phase HPLC was performed on C18 columns (4.6 × 50 mm, 3 μm, Phenomenex) in a model LC-2010A system (Shimadzu). Solvent A was 0.045% TFA in H_2O; solvent B was 0.036% TFA in acetonitrile. Elution was carried out with linear 5–95% gradients of solvent B into A over 15 min at 1 mL/min flow rate, with UV detection at 220 nm.

2.10. Transmission Electron Microscopy (TEM)

Soluble and pre-aggregated (24 h at 37 °C) 1 μM $A\beta_{1-42}$ was dissolved in Ham's F12 medium and incubated in the presence/absence of 5 μM CTerm at 37 °C during 24 h for assembly and disassemble assays. Samples of aggregated peptides obtained as described above were placed onto carbon-coated 200 mesh copper grids and incubated for 5 min. The grids were washed with distilled water and negatively stained with 2% (*w*/*v*) uranyl acetate for 2 min. Micrographs were obtained in a JEM-1010 (JEOL) transmission electron microscope operated at 80 kV accelerating voltage and equipped with an Orius CCD camera.

2.11. Cell Viability Assay by MTT Reduction

A human neuroblastoma cell line (SH-SY5Y cells) was seeded in poly-L-lysine coated 96-well plates at a concentration of 2×10^4 cells/well. Soluble and pre-aggregated (24 h at 37 °C) 1 μM $A\beta_{1-42}$ was dissolved in Ham's F12 medium and incubated in the presence/absence of 5 μM CTerm at 37 °C during 24 h for assembly and disassemble assays. After they were ready the samples were added. Cells were treated with the different samples during 24 h at 37 °C. Cell viability was tested by 3-(4,5-dimethylthiazol-2-yl)-2,5-diphenyltetrazolium bromide (MTT) reduction. 10% *v*/v of MTT stock solution (5 mg/mL) was added. After 2 h the media was replaced with 100 μL of dimethylsulfoxide. MTT absorbance was determined in an Infinite 200 multiplate reader

at A540 nm and corrected by A650 nm. Data are shown compared to untreated controls (100%).

2.12. $A\beta_{1-42}$ Binding to Neuronal Processes

Primary cultures were carried out as previously reported [4]. The procedure was previously approved by the Ethics Committee of the Institut Municipal d'Investigacions Mèdiques-Universitat Pompeu Fabra (EC-IMIM-UPF). Cortical neurons were isolated from 18-day-old OF1 mouse embryos. The brain was removed and the cortex aseptically dissected on ice-cold Hanks' balanced salt solution supplemented with 4.5 g/L glucose and trypsinized for 17 min at 37 °C. In order to eliminate rests of the trypsinization medium and to disaggregate the cells, the cell solution was washed thrice in Hanks' balanced salt solution+glucose and mechanically dissociated. Then, cells were seeded on poly-D-lysine coated coverslips in 24 well-plates with DMEM medium plus 10% horse serum at 10^5 cells/well. Once neurons were attached to the polylysinated wells (2 h), the seeding medium was removed and Neurobasal medium was added containing 2% B27 supplement, 1% GlutaMAX and 1% penicillin/streptomycin. On day 3 of *in vitro* culture, cells were treated with 2 μM 1-β-D-arabinofuranosylcytosine for 24 h to eliminate glia. Primary cortical neurons were used at day 10 [15]. Cells were treated for 10 min at room temperature in mild agitation with 10 μM HiLyte Fluor488 labelled human $A\beta_{1-42}$ ($fA\beta_{1-42}$) preformed in the presence/absence of 20 μM CTerm. After three washes with phosphate-buffered saline (PBS) cells were incubated on ice with 75 μg/mL red concanavaline in neurobasal medium for 20 min. Then cells were washed again in cold PBS and fixed in 4% paraformaldehyde in PBS before mounting. Images were obtained in a SP5 Leica confocal microscope using 40× objective. Image fluorescence analysis was performed using Image J software.

2.13. Statistical Analysis

Data are expressed as the mean ± SEM of the values from the number of experiments as indicated in the corresponding figures. Student's *t*-test or one-way analysis of variance (ANOVA) with Bonferroni multiple comparisons test were used for statistical analyses.

3. Results

3.1. Albumin Binds Aß With Higher Affinity Than Clusterin

Clusterin is known to bind and to inhibit Aβ aggregation [16], in fact some polymorphisms that cause the dysfunction of this protein are a major risk factor for late onset AD [19]. We used $A\beta_{1-42}$ in *in silico* and *in vitro* experiments because it is the most aggregation-prone species of Aβ peptide and, therefore the most neurotoxic in humans [55]. The comparison of the binding affinities of the clusterin peptides and the CTerm to both the alpha and beta conformations of the $A\beta_{1-42}$ (Fig. 1C) shows that the four combinations have relatively acceptable ΔG values. Still, albumin's CTerm peptide systematically obtained significantly better scores ($p < .001$) for the global distribution of all poses. This observation suggests that the CTerm peptide can bind to the $A\beta_{1-42}$ peptide with an affinity equal or possibly higher than clusterin.

3.2. In silico Analysis of $A\beta_{1-42}$-CTerm Interaction

A peptide region of human albumin that had been previously identified with iFRAG [39], was predicted to bind to $A\beta_{1-42}$. The iFRAG method predicts putative fragments that participate in the interface of an interaction through the search for similar sequences of known interactions. We run iFRAG with the albumin and clusterin sequences interacting with the sequence of the $A\beta_{1-42}$ peptide. We obtained several fragments of clusterin and human albumin that would putatively interact with $A\beta_{1-42}$. We selected the high score fragments from iFRAG and aligned the sequences with CLUSTAL [56]. The alignment showed 40% similarity and >25% identity, which increased to >70% on a short stretch of 7 amino-acids [39]. The analysis showed that both proteins share a common sequence located at the albumin's CTerm [39]. The CTerm domain has 35 amino acids (AETFTFHADICTLSEKERQIKKQTALVELVKHKPK) and shows high sequence similarity to clusterin (QNAVNGVKQIKTLIEKTN EERKTLLSNLEEAKKKK) [39].

Here, the binding affinity of the CTerm peptide was computationally evaluated against its regular partner (CTerm-lid) and $A\beta_{1-42}$ in its α and β conformations (Fig. 2A). The score distributions obtained from the generated decoys (Fig. 2B) suggest a slightly higher affinity for the α conformation of $A\beta_{1-42}$ than for the β, albeit far from the affinity to its normal molecular partner. Interestingly, the CTerm peptide seems to trigger strong conformational changes when binding to the $A\beta_{1-42}$ peptide. While binding to the peptide in the α conformation translates into changes between the relative position of the two α-helices, binding to the peptide in the β conformation seems to result in a break of the β configuration that might affect the pairing with other $A\beta_{1-42}$ peptides. The evaluation of the individual contribution of each residue of the CTerm peptide to the binding with $A\beta_{1-42}$ (Fig. 2C) shows the involvement of residues located throughout the entire peptide, suggesting the need for the full peptide for the recognition of its binding partners. When we analyzed the top 5 best scored decoys (Fig. 2D), we observed a very similar binding configuration. These configurations compete directly with the natural helix-loop-helix segment (CTerm-lid) to which the CTerm binds. All the data concerning the docking analysis can be found at https://github.com/structuralbioinformatics/amyloid/tree/master/albumina. A video showing the docking of the CTerm with $A\beta_{1-42}$ is available at https://github.com/structuralbioinformatics/amyloid/raw/master/albumina/images/albumina_top5_overlap.mp4.

To further confirm the different behaviour of the α and β conformations, we docked CTerm and clusterin to the described α-β transition state structure (PDB ID: 1Z0Q) and compare it with the results obtained for the α (PDB ID: 1IYT) and the β (PDB ID: 5OQV) conformation (Fig. S4). This comparison also allows to compensate for the difference in crystallization solvents used between 1IYT and 1Z0Q. As expected from its described condition as transition state, 1Z0Q mostly behaves as an intermediate between the two conformations, the only exception being the RosettaScore evaluation. This fact is not that surprising considering that some of the same metrics that define entry quality in the PDB do affect the scoring provide by Rosetta. The differences in ddG between the binding to albumin or clusterin in 1Z0Q are lower than those we obtained for 1IYT or the β conformation. However, it is still within the range to support that albumin can bind to the Aβ peptide with at least the same or better affinity than clusterin.

3.3. In vitro Analysis of $A\beta_{1-42}$-CTerm Interaction

We synthesized the CTerm as explained in the Methodology Section. The CD mean residue molar ellipticity of the CTerm is shown in Fig. S5. In solution, the peptide shows α-helical distinct features (minima at 204 and 223 nm), with α-helix secondary structure content of 56%. SDS micelles (20 mM detergent) used as helical inducer, increases the propensity of the CTerm secondary structure to 90%, with minima at 206 and 223 nm and a maximum at 192 nm.

Next, we showed the anti-aggregant properties of the CTerm on $A\beta_{1-42}$. CTerm was used at 5 μM, which is the physiological concentration found in human CSF. The hydrophobicity analysis of the species present in several mixtures by reversed-phase chromatography (Fig. 3A) reveals several species. At early elution times (left of the chromatograph), the specific peaks due to the presence of $A\beta_{1-42}$ oligomers are absent when the CTerm is present. In addition, we observed that the CTerm shifts the elution profile to the left, towards more hydrophilic species in the presence of $A\beta_{1-42}$ oligomers when compared with the elution profile of $A\beta_{1-42}$ alone (Fig. 3A,a). This behavior indicates that the CTerm prevents the assembly of oligomeric species. Moreover, the

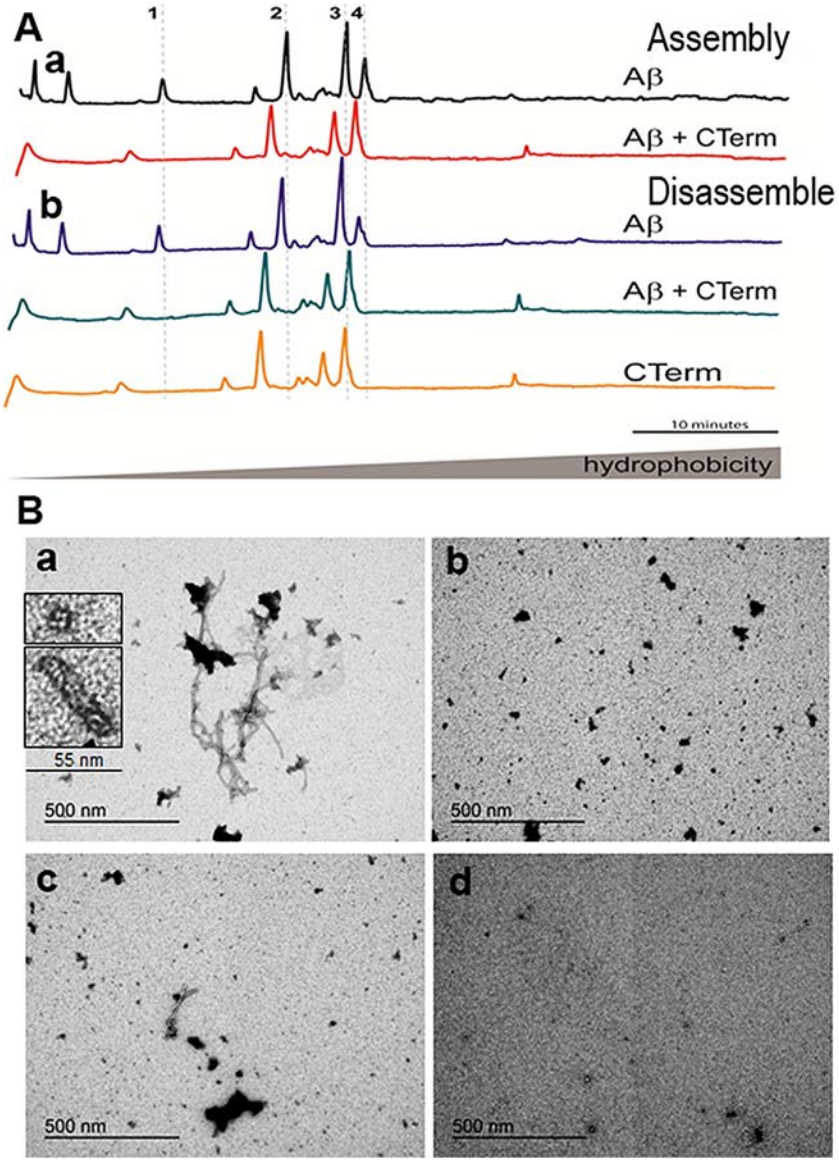

Fig. 3. Effect of the CTerm on $A\beta_{1-42}$ assembly and disassemble *in vitro*. Soluble or aggregated 1 μM $A\beta_{1-42}$ and 1 μM $A\beta_{1-42}$ + 5 μM CTerm were incubated for 24 h to allow soluble Aβ assembly or fibrillar Aβ disassemble. A) Fractions eluted by reverse-phase chromatography. In the central part of the graph are the peaks of the high molecular weight fibrils and on the left the peaks that correspond to low molecular weight oligomers. Representative peaks in terms of hydrophobicity: 1, peak corresponding to $A\beta_{1-42}$ oligomers; 2, 3, and 4, peaks that shift their hydrophobicity in the presence/absence of $A\beta1_{-42}$ fibrils. A,a) Aggregation assay performed with soluble $A\beta_{1-42}$. A,b) Disassemble assay performed with aggregated $A\beta_{1-42}$. Data are from a representative experiment. B) TEM images of aggregation assays. B,a) 1 μM $A\beta_{1-42}$ aggregated for 24 h. Insets correspond to oligomers and protofibrils. B,b) 1 μM $A\beta_{1-42}$ + 5 μM CTerm aggregated for 24 h. B,c) Aggregated 1 μM $A\beta_{1-42}$ + 5 μM CTerm incubated for 24 h. B,d) CTerm alone incubated for 24 h. Representative images are shown.

CTerm was also able to disassemble preformed $A\beta_{1-42}$ aggregates of high (fibrils) and low (oligomers) molecular weights (Fig. 3A,b).

Three peptides of the same size as the CTerm (termed X, Y, Z) were randomly generated to use as controls. We found that the three peptides favour Aβ aggregation and stabilize the pre-existing oligomers and fibrils. The results obtained with Peptide Y, as a representative experiment, are shown in Fig. S6. This pattern of interaction between Aβ and different peptides is expected since it has been reported that the binding of Aβ to proteins can act as seeds for amyloid aggregation and stabilization of fibrils [57–60].

Furthermore, the anti-aggregant properties of the CTerm were studied by TEM (Fig. 3B). When $A\beta_{1-42}$ was incubated alone for 24 h, we observed the presence of the typical amyloid unbranched fibrils (Fig. 3B,a), oligomers and protofibrils (inset in Fig. 3B,a). Upon co-incubation of $A\beta_{1-42}$ with the CTerm, amorphous aggregates were the only structures present (Fig. 3B,b). To study the disassemble ability of the CTerm, when $A\beta_{1-42}$ was prepared as in Fig. 3B, and was incubated for 24 h with the CTerm, small fibrils and amorphous aggregates were observed (Fig. 3B,c). The interference of CTerm in the analysis was discarded because no aggregates were observed when the CTerm was incubated alone (Fig. 3B,d). These results are in agreement with those obtained in the experiment presented in Fig. 3A and Fig. S7.

3.4. CTerm Protects Neurons against Amyloid Neurotoxicity

We also studied the effect of the CTerm on Aβ-induced neurotoxicity on a human neuroblastoma cell line. These studies have been performed with soluble $A\beta_{1-42}$ incubated in the presence/absence of the CTerm for 24 h *in vitro*. Later, the oligomers were added to cells for 24 h (Fig. 4A). A significant protection was observed when $A\beta_{1-42}$ aggregates were preformed in the presence of the CTerm ($p < .05$). Since Aβ aggregates, particularly oligomers, bind to the neuronal membrane impairing its

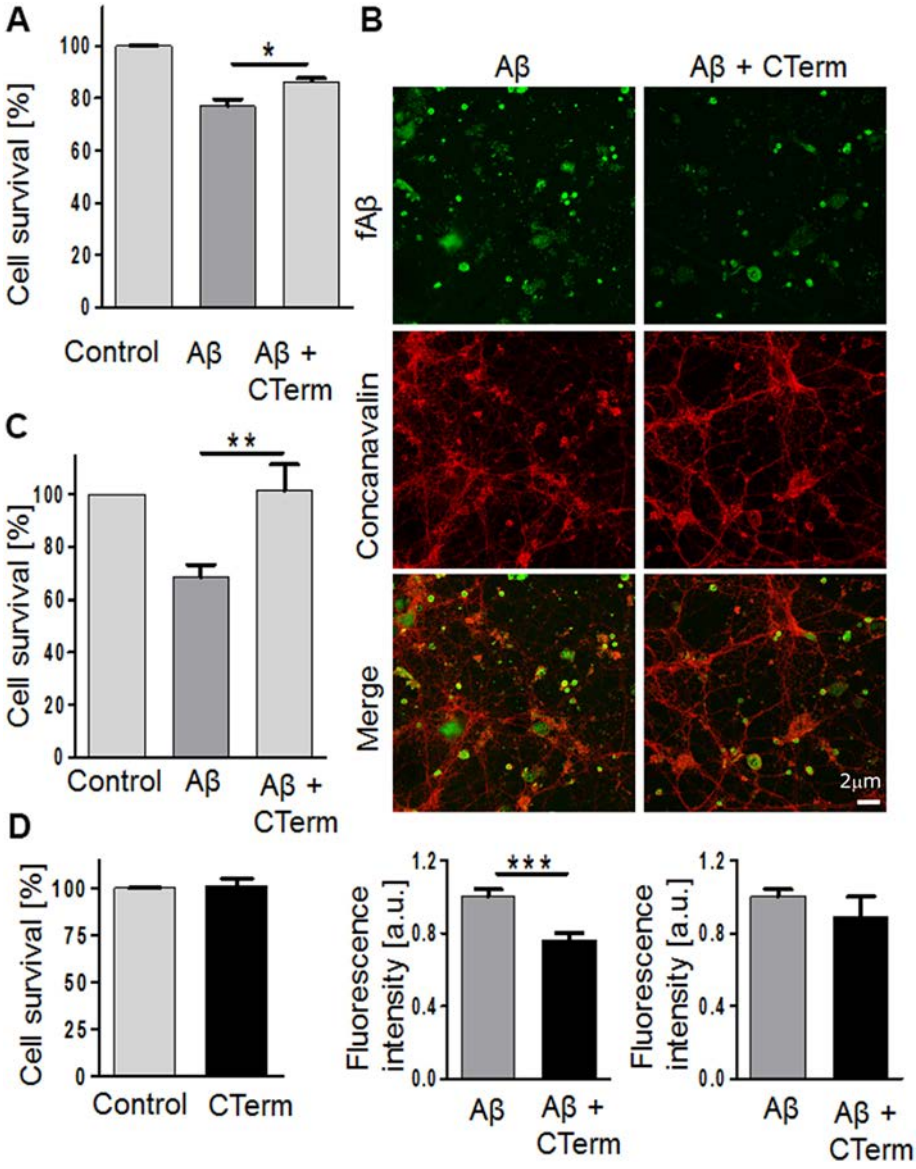

Fig. 4. Effect of the CTerm on Aβ-induced neurotoxicity *in vitro*. A) Human neuroblastoma cells were treated with 1 μM $A\beta_{1-42}$ or 1 μM $A\beta_{1-42}$ + 5 μM CTerm, which were previously incubated for 24 h to allow the assembly of Aβ. Cell viability was assayed by MTT reduction after 24 h. Data are the mean ± SEM from 5 independent experiments performed by duplicate. * $p < .05$ and ** $p < .01$. B) Mouse cortical neurons were incubated with aggregated 10 μM $fA\beta_{1-42}$ and 10 μM $fA\beta_{1-42}$ + 20 μM CTerm for 10 min. Binding of Aβ aggregates to the membrane was evaluated by colocalization with membrane markers (concanavalin A staining). Representative images of $fA\beta_{1-42}$ (green) and concanavalin A (red). The quantification analysis of fluorescence intensity of $fA\beta_{1-42}$ was normalized by concanavalin A (bottom, left). Concanavalin A fluorescence was also independently analyzed (bottom, right). Data are the mean ± SEM of 8 replicates. *** $p < .001$. C) Human neuroblastoma cells were treated with 1 μM $A\beta_{1-42}$ and 1 μM $A\beta_{1-42}$ + 5 μM CTerm, aggregates that were previously incubated for 24 h to allow Aβ disassemble by the CTerm. Cell viability was assayed by MTT reduction after 24 h. Data are the mean ± SEM from 8 independent experiments performed by duplicate. * $p < .05$ and ** $p < .01$.

normal function, we studied the binding of $A\beta_{1-42}$ aggregates formed in the absence/presence of the CTerm to primary cultures of cortical neurons. We used these cell cultures to study the binding of the $A\beta_{1-42}$ aggregates to the surface of neurites mirroring what happens *in vivo*. Experiments were run with concanavalin A, a membrane marker, and a fluorescent $fA\beta_{1-42}$ peptide to study their colocalization (Fig. 4B). Cortical neurons treated with $fA\beta_{1-42}$ aggregates (at 10 μM to allow its visualization) showed higher binding to the membrane throughout the neurite network than oligomers formed in the presence of the CTerm. Fluorescence was quantified and the aggregates of $fA\beta_{1-42}$ formed in the presence of the CTerm showed a 25% reduction in binding to neuronal membranes ($p < .001$; Fig. 4B) while the staining for concanavalin was not modified.

Finally, we prepared $A\beta_{1-42}$ aggregates for 24 h *in vitro*. Then, they were incubated with the CTerm *in vitro* for 24 h in order to disassemble the oligomers. Later, human neuroblastoma cells were challenged with these samples for 24 h (Fig. 4C). $A\beta_{1-42}$ aggregate-induced neurotoxicity was significantly impaired when the $A\beta_{1-42}$ aggregates were pre-incubated with the CTerm ($p < .01$; Fig. 4C). The CTerm alone had no effect on cell viability (Fig. 4D).

4. Discussion

In order to elucidate the albumin domain where the anti aggregant Aβ property is located, we determined the regions of human albumin that could interact with Aβ using the iFRAG procedure [39]. In our previous work we had compared the sequence of clusterin, a well-known Aβ binding protein [16] whose polymorphisms are risk factors for late onset AD [19] with that of albumin. We found that the albumin CTerm has >40% similarity (70% identity on a short 7-residue stretch) with

clusterin, and therefore we focused our study on the properties of this fragment. In the present work we show *in silico* evidence that the CTerm peptide produces conformational changes on $A\beta_{1-42}$ upon binding. This interaction might impair $A\beta_{1-42}$ conformation into β sheets preventing oligomer and fibril formation. These predictions were confirmed *in vitro* by reversed-phase chromatography and electron microscopy. Moreover, the *in silico* results that suggest a change of the β-sheet $A\beta_{1-42}$ structure fit with the ability of the CTerm to induce disassemble of aggregated $A\beta_{1-42}$, data that we obtained by reverse phase chromatography and electron microscopy.

As expected, the CTerm at physiological CSF concentration was able to protect neurons against $A\beta_{1-42}$ neurotoxicity. These results are in agreement with our findings of decreased binding of Aβ aggregates to neuronal membranes when the CTerm is co-incubated with Aβ. Since AD is proposed to begin with the insidious interference of Aβ oligomers on synaptic activity [3,4], we consider that this significant reduction in neurotoxicity and binding of Aβ aggregates to neuronal membranes is reinforcing the protective role of albumin CTerm in AD.

The experimental results in this work highlight the ability of the program iFrag to predict new binding sites for medical relevant targets, for example providing the new binder CTerm for Aβ peptides. Despite previously described interactions between albumin and Aβ peptides, CTerm is a non-exposed region of the albumin and, as such, this site had been dismissed on the prediction of the interaction by other programs. This work confirms that iFrag had successfully identified a fully new binder for Aβ peptides capable of avoiding its aggregation.

Finally, the interest in clusterin and proteins that share common sequences and Aβ binding properties is based on the effect of subtle changes in their sequence, as it has been reported for clusterin [19], or their concentrations, as it has been reported for albumin [61], which along the life of an individual can produce a lack of protection yielding to AD onset after 65 years old.

5. Conclusions

We propose that the CTerm is a key region of albumin that participates in the inhibition of Aβ assembly also favour disassemble of already aggregated Aβ, due to its specific Aβ binding capacity. These findings could set the basis for the design of inhibitory peptides as therapeutic tools for the treatment of AD.

Supplementary data to this article can be found online at https://doi.org/10.1016/j.csbj.2019.06.017.

Acknowledgments

Thanks to Jordi Pujols Pujol for his skillful technical assistance with the RP-HPLC experiments. This work was supported by the Spanish Ministry of Economy and Business through grant Plan Estatal SAF2017-83372-R & SAF2014-52228-R (FEDER funds/UE) to FJM and RV; BIO2017-85329-R to BO; AGL2014-52395-C2 and AGL2017-84097-C2-2-R to D.A.; MDM-2014-0370 through the "María de Maeztu" Programme for Units of Excellence in R&D to "Departament de Ciències Experimentals i de la Salut"; the Chilean Government through Fondecyt 11611065 and AFB170005 to AA, and REDES 180084 to AA and FJM; ISGlobal and IBEC are members of the CERCA Programme, Generalitat de Catalunya.

Declaration of interest

None.

References

[1] Masters CL, Simms G, Weinman NA, Multhaup G, McDonald BL, Beyreuther K. Amyloid plaque core protein in Alzheimer disease and down syndrome. Proc Natl Acad Sci U S A 1985;82:4245–9.
[2] Flament S, Delacourte A, Mann DM. Phosphorylation of Tau proteins: a major event during the process of neurofibrillary degeneration. A comparative study between Alzheimer's disease and Down's syndrome. Brain Res 1990;516:15–9.
[3] Klyubin I, Betts V, Welzel AT, Blennow K, Zetterberg H, Wallin A, et al. Amyloid protein dimer-containing human CSF disrupts synaptic plasticity: prevention by systemic passive immunization. J Neurosci 2008;28:4231–7. https://doi.org/10.1523/JNEUROSCI.5161-07.2008.
[4] Guivernau B, Bonet J, Valls-Comamala V, Bosch-Morató M, Godoy JA, Inestrosa NC, et al. Amyloid-β peptide nitrotyrosination stabilizes oligomers and enhances NMDAR-mediated toxicity. J Neurosci 2016;36:11693–703. https://doi.org/10.1523/JNEUROSCI.1081-16.2016.
[5] Hardy J, Allsop D. Amyloid deposition as the central event in the aetiology of Alzheimer's disease. Trends Pharmacol Sci 1991;12:383–8.
[6] Toro D, Coma M, Uribesalgo I, Guix F, Munoz F. The amyloid β-protein precursor and Alzheimers disease. Therapeutic approaches. Curr Med Chem Nerv Syst Agents 2005;5:271–83. https://doi.org/10.2174/156801505774913053.
[7] De Strooper B, Saftig P, Craessaerts K, Vanderstichele H, Guhde G, Annaert W, et al. Deficiency of presenilin-1 inhibits the normal cleavage of amyloid precursor protein. Nature 1998;391:387–90. https://doi.org/10.1038/34910.
[8] Vassar R, Bennett BD, Babu-Khan S, Kahn S, Mendiaz EA, Denis P, et al. Beta-secretase cleavage of Alzheimer's amyloid precursor protein by the transmembrane aspartic protease BACE. Science 1999;286:735–41.
[9] Qiu Z, Strickland DK, Hyman BT, Rebeck GW. α2-macroglobulin enhances the clearance of endogenous soluble β-amyloid peptide via low-density lipoprotein receptor-related protein in cortical neuron. J Neurochem 2002;73:1393–8. https://doi.org/10.1046/j.1471-4159.1999.0731393.x.
[10] Deane R, Wu Z, Zlokovic BV. RAGE (Yin) versus LRP (Yang) balance regulates Alzheimer amyloid beta-peptide clearance through transport across the blood-brain barrier. Stroke 2004;35:2628–31. https://doi.org/10.1161/01.STR.0000143452.85382.d1.
[11] Prince M, Bryce R, Albanese E, Wimo A, Ribeiro W, Ferri CP. The global prevalence of dementia: a systematic review and metaanalysis. Alzheimers Dement 2013;9:63–75. https://doi.org/10.1016/j.jalz.2012.11.007.
[12] Holtzman DM, Morris JC, Goate AM. Alzheimer's disease: the challenge of the second century. Sci Transl Med 2011;3:77sr1. https://doi.org/10.1126/scitranslmed.3002369.
[13] Solomon B, Koppel R, Hanan E, Katzav T. Monoclonal antibodies inhibit in vitro fibrillar aggregation of the Alzheimer beta-amyloid peptide. Proc Natl Acad Sci U S A 1996;93:452–5.
[14] Ivanoiu A, Pariente J, Booth K, Lobello K, Luscan G, Hua L, et al. Long-term safety and tolerability of bapineuzumab in patients with Alzheimer's disease in two phase 3 extension studies. Alzheimers Res Ther 2016;8:24. https://doi.org/10.1186/s13195-016-0193-y.
[15] Valls-Comamala V, Guivernau B, Bonet J, Puig M, Perálvarez-Marín A, Palomer E, et al. The antigen-binding fragment of human gamma immunoglobulin prevents amyloid β-peptide folding into β-sheet to form oligomers. Oncotarget 2017. https://doi.org/10.18632/oncotarget.17074.
[16] Matsubara E, Soto C, Governale S, Frangione B, Ghiso J. Apolipoprotein J and Alzheimer's amyloid beta solubility. Biochem J 1996:671–9.
[17] Bohrmann B, Tjernberg L, Kuner P, Poli S, Levet-Trafit B, Näslund J, et al. Endogenous proteins controlling amyloid beta-peptide polymerization. Possible implications for beta-amyloid formation in the central nervous system and in peripheral tissues. J Biol Chem 1999;274:15990–5.
[18] Biere AL, Ostaszewski B, Stimson ER, Hyman BT, Maggio JE, Selkoe DJ. Amyloid beta-peptide is transported on lipoproteins and albumin in human plasma. J Biol Chem 1996;271:32916–22. https://doi.org/10.1074/jbc.271.51.32916.
[19] Duguid JR, Bohmont CW, Liu NG, Tourtellotte WW. Changes in brain gene expression shared by scrapie and Alzheimer disease. Proc Natl Acad Sci U S A 1989;86:7260–4.
[20] Ramos-Fernández E, Tajes M, Palomer E, Ill-Raga G, Bosch-Morató M, Guivernau B, et al. Posttranslational nitro-glycative modifications of albumin in Alzheimer's disease: implications in cytotoxicity and amyloid-β peptide aggregation. J Alzheimers Dis 2014;40:643–57. https://doi.org/10.3233/JAD-130914.
[21] Milojevic J, Melacini G. Stoichiometry and affinity of the human serum albumin-Alzheimer's Aβ peptide interactions. Biophys J 2011;100:183–92. https://doi.org/10.1016/j.bpj.2010.11.037.
[22] Milojevic J, Esposito V, Das R, Melacini G. Understanding the molecular basis for the inhibition of the Alzheimer's Abeta-peptide oligomerization by human serum albumin using saturation transfer difference and off-resonance relaxation NMR spectroscopy. J Am Chem Soc 2007;129:4282–90. https://doi.org/10.1021/ja067367+.
[23] Algamal M, Ahmed R, Jafari N, Ahsan B, Ortega J, Melacini G. Atomic-resolution map of the interactions between an amyloid inhibitor protein and amyloid β (Aβ) peptides in the monomer and protofibril states. J Biol Chem 2017;292:17158–68. https://doi.org/10.1074/jbc.M117.792853.
[24] Christenson RH, Behlmer P, Howard JF, Winfield JB, Silverman LM. Interpretation of cerebrospinal fluid protein assays in various neurologic diseases. Clin Chem 1983;29:1028–30.
[25] Ahn S-M, Byun K, Cho K, Kim JY, Yoo JS, Kim D, et al. Human microglial cells synthesize albumin in brain. PLoS One 2008;3:e2829. https://doi.org/10.1371/journal.pone.0002829.
[26] He XM, Carter DC. Atomic structure and chemistry of human serum albumin. Nature 1992;358:209–15. https://doi.org/10.1038/358209a0.
[27] Sugio S, Kashima A, Mochizuki S, Noda M, Kobayashi K. Crystal structure of human serum albumin at 2.5 a resolution. Protein Eng 1999;12:439–46.
[28] Carter DC, Ho JX. Structure of serum albumin. Adv Protein Chem 1994;45:153–203.

[29] Kragh-Hansen U. Structure and ligand binding properties of human serum albumin. Dan Med Bull 1990;37:57–84.
[30] Ghuman J, Zunszain PA, Petitpas I, Bhattacharya AA, Otagiri M, Curry S. Structural basis of the drug-binding specificity of human serum albumin. J Mol Biol 2005; 353:38–52. https://doi.org/10.1016/j.jmb.2005.07.075.
[31] Fanali G, Di Masi A, Trezza V, Marino M, Fasano M, Ascenzi P. Human serum albumin: from bench to bedside. Mol Aspects Med 2012;33:209–90. https://doi.org/10.1016/j.mam.2011.12.002.
[32] Simard JR, Zunszain PA, Ha C-E, Yang JS, Bhagavan NV, Petitpas I, et al. Locating high-affinity fatty acid-binding sites on albumin by x-ray crystallography and NMR spectroscopy. Proc Natl Acad Sci U S A 2005;102:17958–63. https://doi.org/10.1073/pnas.0506440102.
[33] Whitlam JB, Crooks MJ, Brown KF, Veng Pedrrsen P. Binding of nonsteroidal anti-inflammatory agents to proteins—I. Ibuprofen-serum albumin interaction. Biochem Pharmacol 1979;28:675–8. https://doi.org/10.1016/0006-2952(79)90154-0.
[34] Bar-Or D, Rael LT, Lau EP, Rao NKR, Thomas GW, Winkler JV, et al. An analog of the human albumin N-terminus (Asp-Ala-His-Lys) prevents formation of copper-induced reactive oxygen species. Biochem Biophys Res Commun 2001;284:856–62. https://doi.org/10.1006/bbrc.2001.5042.
[35] Stanyon HF, Viles JH. Human serum albumin can regulate amyloid-peptide fiber growth in the brain interstitium: implications for Alzheimer disease. J Biol Chem 2012;287:28163–8. https://doi.org/10.1074/jbc.C112.360800.
[36] Algamal M, Milojevic J, Jafari N, Zhang W, Melacini G. Mapping the interactions between the Alzheimer's Aβ-peptide and human serum albumin beyond domain resolution. Biophys J 2013;105:1700–9. https://doi.org/10.1016/j.bpj.2013.08.025.
[37] Kuo Y-M, Emmerling MR, Lampert HC, Hempelman SR, Kokjohn TA, Woods AS, et al. High levels of circulating Aβ42 are sequestered by plasma proteins in Alzheimer's disease. Biochem Biophys Res Commun 1999;257:787–91. https://doi.org/10.1006/bbrc.1999.0552.
[38] Kuo Y-M, Kokjohn TA, Kalback W, Luehrs D, Galasko DR, Chevallier N, et al. Amyloid-β peptides interact with plasma proteins and erythrocytes: implications for their quantitation in plasma. Biochem Biophys Res Commun 2000;268:750–6. https://doi.org/10.1006/bbrc.2000.2222.
[39] Garcia-Garcia J, Valls-Comamala V, Guney E, Andreu D, Muñoz FJ, Fernandez-Fuentes N, et al. iFrag: a protein–protein interface prediction server based on sequence fragments. J Mol Biol 2017;429:382–9. https://doi.org/10.1016/j.jmb.2016.11.034.
[40] Janin J, Bahadur RP, Chakrabarti P. Protein–protein interaction and quaternary structure. Q Rev Biophys 2008;41:133–80. https://doi.org/10.1017/S0033583508004708.
[41] Wass MN, Fuentes G, Pons C, Pazos F, Valencia A. Towards the prediction of protein interaction partners using physical docking. Mol Syst Biol 2011;7:469. https://doi.org/10.1038/msb.2011.3.
[42] Marín-López MA, Planas-Iglesias J, Aguirre-Plans J, Bonet J, Garcia-Garcia J, Fernandez-Fuentes N, et al. On the mechanisms of protein interactions: predicting their affinity from unbound tertiary structures. Bioinformatics 2018;34:592–8. https://doi.org/10.1093/bioinformatics/btx616.
[43] Šali A, Blundell TL. Comparative protein modelling by satisfaction of spatial restraints. J Mol Biol 1993;234:779–815. https://doi.org/10.1006/jmbi.1993.1626.
[44] Martí-Renom MA, Stuart AC, Fiser A, Sánchez R, Melo F, Šali A. Comparative protein structure modeling of genes and genomes. Annu Rev Biophys Biomol Struct 2000; 29:291–325. https://doi.org/10.1146/annurev.biophys.29.1.291.
[45] Eswar N, Webb B, Marti-Renom MA, Madhusudhan MS, Eramian D, Shen M, et al. Comparative protein structure modeling using MODELLER. Curr Protoc Protein Sci 2007;50:2.9.1–2.9.31. https://doi.org/10.1002/0471140864.ps0209s50 John Wiley & Sons, Inc.
[46] Alford RF, Leaver-Fay A, Jeliazkov JR, O'Meara MJ, DiMaio FP, Park H, et al. The Rosetta all-atom energy function for macromolecular modeling and design. J Chem Theory Comput 2017;13:3031–48. https://doi.org/10.1021/acs.jctc.7b00125.
[47] Berman HM, Kleywegt GJ, Nakamura H, Markley JL. The protein data Bank archive as an open data resource. J Comput Aided Mol Des 2014;28:1009–14. https://doi.org/10.1007/s10822-014-9770-y.
[48] Adams R, Griffin L, Compson JE, Jairaj M, Baker T, Ceska T, et al. Extending the half-life of a fab fragment through generation of a humanized anti-human serum albumin Fv domain: an investigation into the correlation between affinity and serum half-life. MAbs 2016;8:1336–46. https://doi.org/10.1080/19420862.2016.1185581.
[49] Crescenzi O, Tomaselli S, Guerrini R, Salvadori S, D'Ursi AM, Temussi PA, et al. Solution structure of the Alzheimer amyloid β-peptide (1-42) in an apolar microenvironment. Eur J Biochem 2002;269:5642–8. https://doi.org/10.1046/j.1432-1033.2002.03271.x.
[50] Gremer L, Schölzel D, Schenk C, Reinartz E, Labahn J, Ravelli RBG, et al. Fibril structure of amyloid-β(1–42) by cryo–electron microscopy. Science 2017;358:116–9. https://doi.org/10.1126/SCIENCE.AAO2825 (80-).
[51] Kilambi KP, Reddy K, Gray JJ. Protein-protein docking with dynamic residue protonation states. PLoS Comput Biol 2014;10:e1004018. https://doi.org/10.1371/journal.pcbi.1004018.
[52] Nivón LG, Moretti R, Baker D. A pareto-optimal refinement method for protein design scaffolds. PLoS One 2013;8:e59004. https://doi.org/10.1371/journal.pone.0059004.
[53] Louis-Jeune C, Andrade-Navarro MA, Perez-Iratxeta C. Prediction of protein secondary structure from circular dichroism using theoretically derived spectra. Proteins 2012;80:374–81. https://doi.org/10.1002/prot.23188.
[54] Bitan G, Teplow DB. Preparation of aggregate-free, low molecular weight amyloid-beta for assembly and toxicity assays. Methods Mol Biol 2005;299:3–9.
[55] Chang Y-J, Chen Y-R. The coexistence of an equal amount of Alzheimer's amyloid-β 40 and 42 forms structurally stable and toxic oligomers through a distinct pathway. FEBS J 2014;281:2674–87. https://doi.org/10.1111/febs.12813.
[56] Sievers F, Higgins DG. Clustal omega, accurate alignment of very large numbers of sequences. Methods Mol Biol 2014;1079:105–16. https://doi.org/10.1007/978-1-62703-646-7_6.
[57] Muñoz FJ, Inestrosa NC. Neurotoxicity of acetylcholinesterase amyloid beta-peptide aggregates is dependent on the type of Abeta peptide and the AChE concentration present in the complexes. FEBS Lett 1999;450:205–9.
[58] Castillo GM, Lukito W, Wight TN, Snow AD. The sulfate moieties of glycosaminoglycans are critical for the enhancement of beta-amyloid protein fibril formation. J Neurochem 1999;72:1681–7.
[59] Motamedi-Shad N, Monsellier E, Chiti F. Amyloid formation by the model protein muscle acylphosphatase is accelerated by heparin and heparan sulphate through a scaffolding-based mechanism. J Biochem 2009;146:805–14. https://doi.org/10.1093/jb/mvp128.
[60] Shin TM, Isas JM, Hsieh C-L, Kayed R, Glabe CG, Langen R, et al. Formation of soluble amyloid oligomers and amyloid fibrils by the multifunctional protein vitronectin. Mol Neurodegener 2008;3(1):16. https://doi.org/10.1186/1750-1326-3-16.
[61] Llewellyn DJ, Langa KM, Friedland RP, Lang IA. Serum albumin concentration and cognitive impairment. Curr Alzheimer Res 2010;7:91–6. https://doi.org/10.2174/156720510790274392.